01

Two-photon excitation of nitrogen oxide at photofragmentation of nitrobenzene

© A.V. Puchikin[1], Yu.N. Panchenko[1,2], M.V. Andreev[2], I.N. Konovalov[1], V.E. Prokopiev[2]

[1] Institute of High Current Electronics, Siberian Branch, Russian Academy of Sciences,
634055 Tomsk, Russia
[2] Tomsk State University,
634050 Tomsk, Russia

e-mail: apuchikin@mail.ru

Received December 11, 2023
Revised January 09, 2024
Accepted January 16, 2024

The results of a study of the temporal and spectral characteristics of the fluorescence of nitric oxide NO $A^2\Sigma$ obtained under dual-frequency laser action with nitrobenzene $C_6H_5NO_2$ are presented. The physical mechanism for the appearance of fluorescence from the electronic level of NO $A^2\Sigma$, $v'(0)$, caused by two-photon excitation of the electronic transition NO $A^2\Sigma - X^2\Pi$, $v'v''$ $(0, 1)$ by laser radiation (472 nm) of femtosecond duration, is shown. In this case, vibrationally excited NO $X^2\Pi$, $v''(1)$ molecules appear as photofragments of nitrobenzene after interaction with laser radiation of a KrF-laser (248.3 nm) of nanosecond duration. It is noted that registration of the fluorescent signal for this experimental setup is observed at a femtosecond pulse intensity of $\sim 300\,GW/cm^2$.

Keywords: photofragmentation, two-photon absorption, nitro compound, fluorescence.

DOI: 10.61011/EOS.2024.01.58283.6-24

Introduction

Remote optical methods for detection of various harmful and hazardous vapors in atmospheric air currently exist and are being developed. When remote detection of remote objects or the target air space in atmosphere, optical (laser) probing and ranging systems are used [1,2]. Absorption bands of most volatile nitroaromatic and organic substances are within an ultraviolet range of 200–300 nm [3,4]. Receipt of an intense fluorescent signal in photoexcitation of compounds with complex molecular structure during exposure to single laser pulses is limited by many degrees of freedom of the molecules of interest. In our point of view, photo-fragmentation of the main molecule followed by laser-induced fluorescence of its vibrationally-excited fragments (PF-LIF) is the most efficient and sensitive optical method for detection of these substances. It should be noted that this optical method is used to identify the original substance by indirect features, i.e. by the presence of narrow spectral fluorescence bands of their main fragments. For efficient utilization of the single-frequency PF-LIF method, it is necessary to provide some conditions for interaction between the probing emission and the substance: the test molecules shall have high absorption cross-section for the employed emission wavelength, absorption shall result in molecule dissociation, the resulting photofragments shall be suitable for further laser-induced fluorescence (LIF), emission pulse duration shall correspond to the duration of all successive processes [5].

Studies [6–8] show that the single-frequency PF-LIF method may be used to detect volatile organic compounds containing a C-NO_2 nitrogroup in the atmosphere. These studies used narrow-band emission at 226, 236 and 247 nm corresponding to resonant electronic-vibrational transitions of NO $A^2\Sigma$-X^2P,$v'v''(0, 0)$, $v'v''(0, 1)$ and $v'v''(0, 2)$ photofragments. For all experiments, the fluorescence signals were recorded in a short-wavelength region of NO $A^2\Sigma$-X^2P, $v'v''(0, 0)$ at 226 nm.

The main issue of detection of a low-volatile nitrocompound vapor phase is that formation of vibrationally-excited NO $X^2\Pi$, $v'' > 0$ at the photo-fragmentation stage is inefficient for the further LIF process. Further studies were associated with increase in sensitivity and efficiency of the PF-LIF method. Ultraviolet laser sources were used at different wavelengths both for the photo-fragmentation stage and further fragment probing. Double-frequency laser interaction was used to increase NO $X^2\Pi$, $v''(2)$ concentration, that occurs in photo-fragmentation, for the LIF process and also as a subject of investigation of efficient NO $X^2\Pi$, $v''(2)$ population time [9–11].

A more short-wavelength emission of 222.1 nm of the KrCl excimer gas-discharge laser in interaction with nitrobenzene that have been previously used by us made it possible to increase the efficiency of population of vibrationally-excited NO $X^2\Pi$, $v''(2-4)$ in photofragmentation of the main R-NO_2 molecules and of secondary PF-LIF of larger NO_2 fragments within the emission pulse duration [12]. However, far-ultraviolet (UV-C) lasers may not be always used for atmospheric air probing, because the ultraviolet (UV) laser propa-

gation in the atmosphere is limited due to collisional de-excitation and absorption by O_2, O_3 and N_2 gases. Oxygen photo-dissociation may result in formation of O_3 molecules that have the Hartley spectral band with strong absorption at 210−290 nm ($\sigma_{abs} = 1.12 \cdot 10^{-17}$ cm^2/mol for 253.65 nm) [13]. Therefore the exploratory studies of the efficient interaction between laser emission and complex organic compounds using nitrocompounds are still important.

For investigation of the LIF processes, when single-photon excitation is not sufficient due to high energy distance between the ground state and excited state of a molecule, multiphoton interactions are used. Thanks to high emission intensity, laser systems with ultrashort pulse duration allow the induced nonlinear photo-dissociation and excitation of he test molecules to be carried out easily. Whilst the emission pulse energy remain low compared with the laser emission for multiphoton nanosecond-range processes [14–17].

The study describes the investigation of the time and spectral responce characteristics of fluorescence of vibrationally-excited nitrogen oxide fragments formed by photo-dissociation of aromatic nitrobenzene (NB) compound. For the first time, the double-frequency interaction between laser emission and nitrocompound is analyzed by the optic spectral analysis method: photo-fragmentation of the main molecule followed by LIF of its NO fragments with two-photon absorption (photo-fragmentation-two-photon-absorption-laser-induced-fluorescence, PF-TPALIF). Substantial share of population of vibrationally-excited NO $X^2\Pi$, $v''(1)$ is obtained through the nitrobenzene stage in interaction with the nanosecond pulse of KrF excimer laser with a central wavelength of 248.3 nm. For the LIF process, two-photon excitation of NO $A^2\Sigma-X^2\Pi$, $v'v''$ (0,1) molecules was carried out using 472 nm fs-laser emission and further recording of NO $A^2\Sigma-X^2\Pi$, $v'v''$ (0,2) band fluorescence.

Experimental equipment and measurement techniques

The experiment on interaction between laser emission and NB used two laser sources: photo-fragmenting LS1 and probing LS2. General specifications of the sources are listed in the Table.

The first NB photo-fragmentation stage used the nanosecond laser emission of 248.3 nm KrF laser (IHCE SB RAS, model ELF) with an exposure intensity of 2 MW/cm^2. Numerical model, optical and electrical circuit of the KrF laser are described in [18–20]. Further TPALIF stage of NO $A^2\Sigma-X^2\Pi$, $v'v''$ (0, 1) used 472 nm femtosecond second harmonic (SH) laser emission that was generated by Ti:Sa tunable laser system (Avesta, model 480).

For the femtosecond laser system flow-chart, see Figure 1. 944 nm 50−70 fs emission was induced by the master generator, then, after passing the stretcher, the pulse duration increased up to 100 ps and then the energy was raised up to 12 mJ in feedback multipass Ti:Sa amplifier. The next stage included pulse duration compression up to 50 fs in the compressor consisting of two diffraction gratings. For second harmonic generation of the 472 nm primary emission, KDP type I laser 2 mm in thickness and axes orientation $\theta = 41^\circ$ and $\phi = 45^\circ$ was used.

Two-photon excitation of the NO $A^2\Sigma-X^2\Pi$, $v'v''$ (0,1) absorption band was carried out at an intensity of 300 GW/cm^2 of 472 nm laser emission using additional compression of the initial beam by spherical lens L1 $f = 500$ mm in the region of interest. Emission of both laser sources was directed on along one optical axis into the gas cell with NB through the M1 248.3/472 nm dichroic mirror (Thorlabs, BB1-E01). A controlled two-channel pulsed oscillator (Digit-EL, PG-872) was used for synchronization and delay time parameters of the spectrum equipment and laser systems.

The optical diagram of the experimental setup is shown in Fig. 2. interaction between the laser emission and saturated NB vapors ($\sim$ 244 ppm) took place in a stainless steel gas cell at room temperature 298 K. KU-1 quartz windows were placed at the cell ends to transmit the induced 250 nm fluorescence of nitrogen oxide with minimum loss. The cell was preliminary evacuated by a turbomolecular pump (ILMVAC, Turbo-V 81-AG) to 10^{-5} Pa. The test NB vapor/air mixture (1 atm) was admitted into the cell by a mass flow controller (MKS, GE50A013500RMV020).

NO $A^2\Sigma-X^2\Pi$, $v'v''$ (0,2) fluorescence was recorded at right angle to the incident emission. Quartz lens L2 collected the scattered emission and formed an exposure region image on the monochromator entrance slit. Scattered light suppression and spectral selection of the backscattered signal were performed by a monochromator (Shamrock, SR500) with a focal distance of 500 mm and additional narrow-band filter F (Semrock, Hg 01-254-25, $T \sim 60\%$ at 250 nm). Time and amplitude characteristics of the emission pulse were recorded by iStarICCD camera (AndorTechnology, DH720-18F-03) with a resolution lower than 5 ns with photocathode quantum efficiency $\sim$ 10% at 240−250 nm. The recorded experimental spectra of NO fluorescence were compared using LIFBASE, LIFSIM spectrum simulation software products [21,22]. Laser emission energy was measured by a calorimeter (Gentec-EO).

Results and discussion

Nitrobenzene photo-fragmentation

Nitrobenzene is classified as an aromatic compound containing one NO_2 nitrogroup. The cell experiments used a saturated NB vapor concentration of 244 ppm that was calculated using the Antoine equation and corrected by an

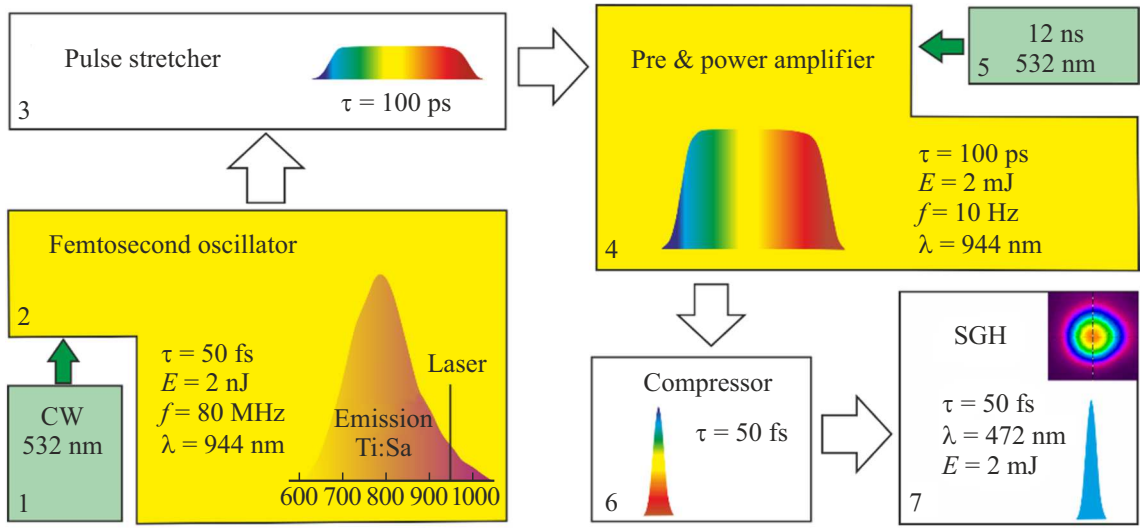

Figure 1. fs-laser flow-chart: 1 — continuous pumping laser of the master oscillator, 2 — master oscillator of fs-pulses, 3 — stretcher, 4 — feedback multipass amplifier, 5 — pumping pulsed laser, 6 — compressor, 7 — second harmonic generator.

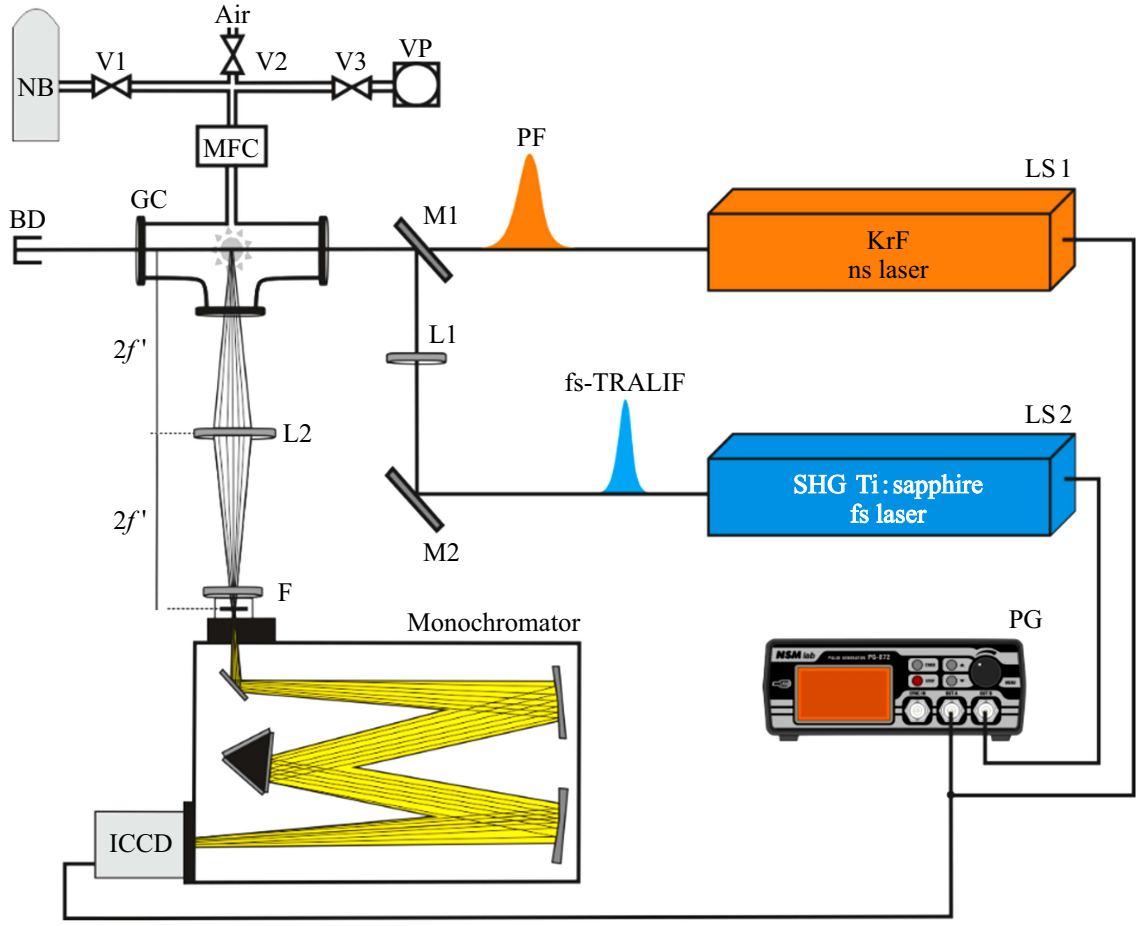

Figure 2. Experimental setup of PF-TPALIF NB: LS1 — ns-laser, LS2 — fs-laser, PG — pulsed delay generator, M1 — dichroic mirror, M2 — narrow-band mirror, GC — gas cell, BD — beam absorber, F — narrow-band filter, L1 — f-500 mm lens, L2 — f-150 mm collecting lens, Monochromator — monochromator with a focal length of 500 mm, ICCD — intensified CCD camera, MFC — admission controller, V1–V3 — motor-operated valves, VP — vacuum pump.

Table 1. Laser source parameters

Type Stage	LS 1—KrF photo-fragmentation	LS 2 — Ti:Sapphire LIF
Wavelength,nm	248.3	472
Pulse duration(FWHM)	10 ns	50 fs
Line width	10 pm	6.5 nm
Maximum energy, mJ	100	< 5
Repetition frequency , Hz	50	10
divergence, mrad	< 0.8	0.1
Beam dimensions, mm	5×10	Ø 10

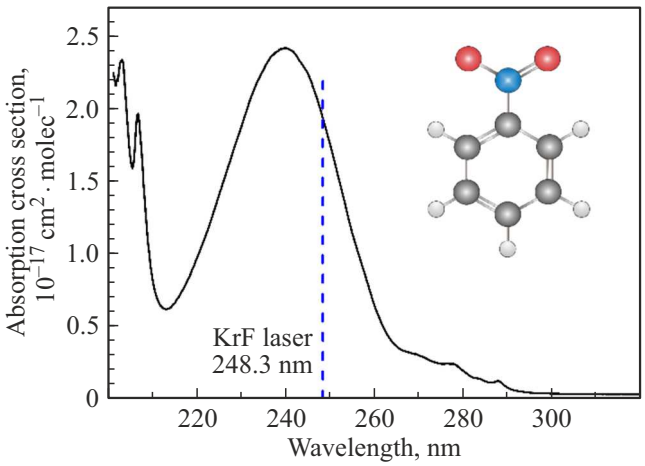

Figure 3. Interaction between the 248.3 nm laser emission and nitrobenzene. Experimental cross-section of nitrobenzene absorption (black solid curve) [24]; KrF laser emission (blue vertical dashed line).

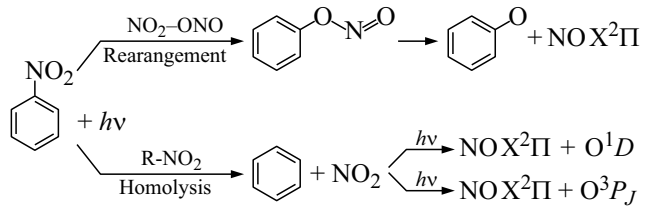

Figure 4. Nitrobenzene bond breakage by way of nitro-nitrate isomerization and homolysis.

air temperature of 298 K [23]:

$$\mathrm{Ln}(P) = ANTA - \left(\frac{ANTB}{T + ANTC}\right), \qquad (1)$$

where P is the pressure in mm Hg, $ANTA$, $ANTB$, $ANTC$ are the Antoine constants, T is the temperature in K. The maximum interaction cross-section of nitrobenzene is in the UV range (Figure 3).

For the NB photo-fragmentation, the narrow-band KrF excimer laser emission was used at 248.3 nm. Photokinetic reactions are represented as follows:

$$C_6H_5NO_2 + h\nu \rightarrow C_6H^5O + NO, \qquad (2)$$

$$C_6H_5NO_2 + h\nu \rightarrow C_6H_5 + NO_2, \qquad (3)$$

$$C_6H_5NO_2 + h\nu \rightarrow C_6H_4 + HONO, \qquad (4)$$

$$C_6H_5NO_2 + h\nu \rightarrow C_6H_5NO + O. \qquad (5)$$

For further LIF process, the model addresses reactions (2) and (3) to achieve vibrationally-excited states of NO $X^2\Pi$, $v'' > 1$ at the photo-fragmentation stage. Figure 4 schematically shows the main channels of NO $X^2\Pi$, v'' formation during single-frequency interaction between nitrobenzene and laser emission. In the first case for photoreaction (2), the C-NO_2 bond breakage is implemented through nitro-nitrate isomerization into a low-energy transient state followed by O-NO bond breakage. NO molecules formed through this channel have the population distribution by NO $X^2\Pi$, $v''(0/1/2)-(0.81/0.11/0.04)$ levels within the full fragmentation time ~ 30 ns. In second case for photoreaction (3), C-NO_2 dissociation flows at high formation rate of NO_2 fragments during the time in units of nanoseconds [11,25,26]. Also, the NB photo-fragmentation process shall include the quantum yield of NO $X^2\Pi$ molecules. Study [27] has experimentally shown that the quantum yield ratio of $NO_2/NO(v)$ fragments varies from 5.9/1 to 3.7/1 with emission wavelength increase from 222 nm to 240 nm. The interaction cross-section for 248.3 nm emission with nitrogen dioxide ($\sigma_{NO_2} = 7.66 \cdot 10^{-21}$ cm^{2}mol^{-1}) is considerably lower compared with nitrobenzene ($\sigma_{NB} = 1.93 \cdot 10^{-17}$ cm^{2}mol^{-1}). Therefore, the contribution to the total concentration of NO $X^2\Pi$, $v''(1)$ from the secondary photo-fragmentation of NO_2 will be negligible [28]. Hence, if 248.3 nm is chosen, NO $X^2\Pi$, $v''(1)$ state population will be about 15%, which is much higher than the population of the associated atmospheric nitrogen oxide according to the Boltzmann distribution by vibrationally-excited NO $X^2\Pi$, $v''(0/1/2)-1/10^{-4}/10^{-8}$ levels at $T = 300$ K [29].

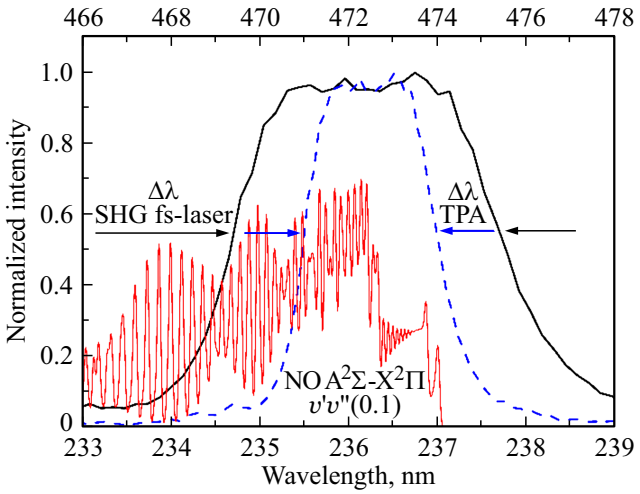

Figure 5. LIFBASE calculated absorption spectrum for NO $A^2\Sigma-X^2\Pi$, $v'v''$ (0,1) at $T_{rot} = 3500$ K (red); second harmonic Ti:Sa laser emission spectrum (black); calculated two-photon absorption (TPA) spectrum (blue).

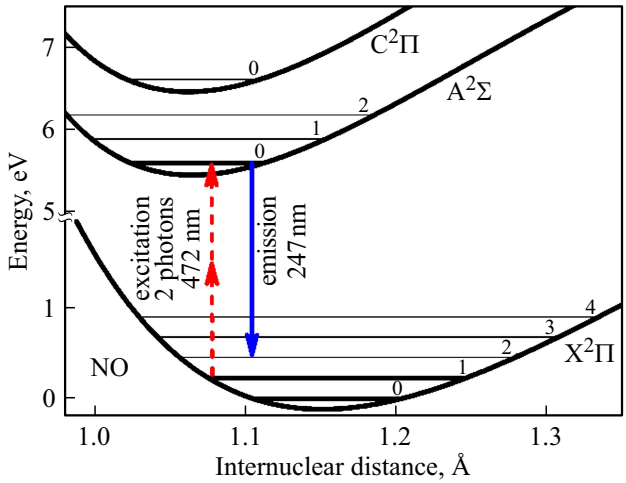

Figure 6. Potential energy curves for NO $A^2\Pi$, C^2P, X^2P.

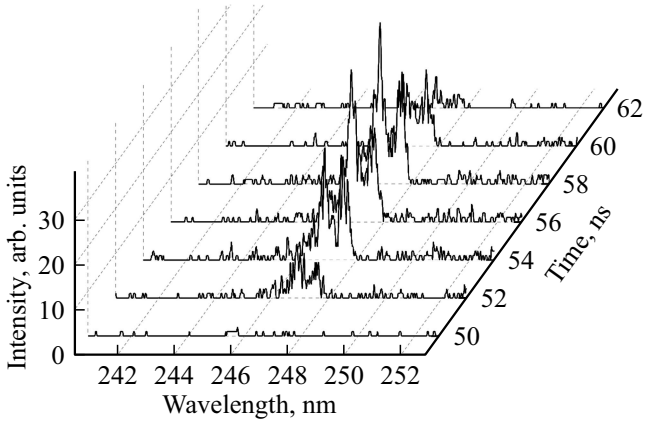

Figure 7. Kinetic series of NO $A^2\Sigma-X^2P$, $v'v''(0, 2)$ fluorescence spectra for the PF-TPALIF process.

Laser-induced fluorescence of nitrogen oxide

The experimental studies of nitrobenzene photofragmentation by 226–280 nm laser emission reported that „hot“ fragments of nitrogen oxide were formed at $T_{rot} = 2400-3700$ K [26,30]. Spectral broadening of the absorption band of nitrogen oxide photofragments will help increase the efficiency of exciting broadband emission. Figure 5 shows the calculated spectrum of two-photon absorption by NO $A^2\Sigma-X^2\Pi$, $v'v''$ (0, 1) molecule at $T_{rot} = 3500$ K (LIFBASE) and second harmonic (SH) laser emission of the tunable Ti:Sa laser. Spectral full width at half maximum (FWHM) of the affecting SH pulse of 472 nm Ti:Sa laser system at 50 fs is equal to 6.5 nm and limited by the bandwidth. Relative to NO $A^2\Sigma-X^2\Pi$, $v'v''$ (0, 1) absorption with two-photon absorption for 236 nm, the spectral width will decrease to 1.64 nm:

$$\Delta\lambda = (TBP\lambda_{236}^2)/(\Delta\tau\, c), \qquad (6)$$

where TBP is the product by the Gaussian pulse bandwidth with a limited bandwidth (0.441 was used), $\Delta\tau$ is the pulse duration, c is the speed of light.

Figure 6 shows the two-photon absorption by the 472 nm band of NO $A^2\Sigma-X^2\Pi$, $v'v''$ (0, 1) and further experimentally recorded fluorescence emission of NO $A^2\Sigma-X^2\Pi$, $v'v''$ (0,2) . Oscillator forces of these electronic transitions in LIFBASE spectrum simulation software were defined for absorption $f_{abs}(0, 1) = 6.077 \cdot 10^{-4}$ and for emission capacity $f_{em}(0, 2) = 6.422 \cdot 10^{-4}$. Fluorescence duration of NO $A^2\Sigma$, v' (0) state in atmospheric air is defined by radiative lifetime 206 ns and decreases to 1.5 ns due to drastic collisional quenching of O_2 at $k_q = (1.6 \pm 0.2) \cdot 10^{-10}$ cm^{3}s^{-1}. For molecular N_2, the quenching constant of NO $A^2\Sigma$, v' (0) is much lower: $k_q = 0.008 \cdot 10^{-10}$ cm^{3}s^{-1} [31,32].

The recorded kinetic series of NO $A^2-X^2\Pi$, $v'v''(0, 2)$ spectra for the PF-TPALIF NO_2 process (Figure 7) show quenching of NO $A^2\Sigma$ state fluorescence by atmospheric gases. fluorescence spectrum was recorded in the 247 nm stokes region relative to absorption 236 nm, where the emission coefficient determined in LIFBASE spectrum simulation software, $A(0, 2) = 1.215 \cdot 10^6$ s^{-1}, is maximum for NO $A^2\Sigma$, $v'(0)$ state compared with the nearby vibrational levels for which $A(0, 0) = 9.802 \cdot 10^5$ s^{-1}, $A(0, 3) = 7.677 \cdot 10^5$ s^{-1}. To avoid potential occurrence of NO $A^2\Sigma$, $v'(0)$ fluorescence as a result of exposure to photo-fragmenting KrF laser, wavelength 248.3 nm with spectral width 10 nm was tuned outside the NO $A^2\Sigma$-$X^2\Pi$, $v'v''(0, 2)$ absorption band envelope. Delay time of the probing laser from the fragmenting laser was set to 50 ns according to the previous data on the maximum population time of NO $X^2\Pi$, $v''(2)$ level [10].

Conclusion

According to the results of these investigations, an innovative spectroscopy method PF-TPALIF has been proposed to determine the population of NO $X^2\Pi$, v'' vibrational levels. Photokinetic processes flowing in complex $C-NO_2$ molecules have been defined . Using nitrobenzene with preliminary photo-fragmentation by UV-C laser emission, population of NO $X^2\Pi$, $v''(1)$ level was achieved for further two-photon interaction. Probing laser emission in the blue spectrum region with a pulse duration of 50 fs and intensity $\sim 300\,GW/cm^2$ results in fluorescence of NO $A^2\Sigma$, $v''(0)$ state due to two-photon absorption at electronic transition NO $A^2\Pi-X^2\Pi$, $v'v''(0,1)$. The advantage of probing with an ultrashort pulse is in the fact that associated photolytic processes occurring during single-photon photo-dissociation are minimized. In this case, both interaction selectivity and linear dispersion of LIF signal caused by noise-induced laser scattering are increased.

Funding

The study was conducted under the state job-order of the Ministry of Science and Higher Education of the Russian Federation (FWRM-2021-0014) and supported by the Development Program of Tomsk State University (Prioritet-2030).

Conflict of interest

The authors declare that they have no conflict of interest.

Author contributions

A.V. Puchikin: concept development, research, writing; Yu.N. Panchenko: administration, text editing, approval of the final version; M.V. Andreev: statistical data processing; I.N. Konovalov: resource provision for the study; V.E. Prokopiev: statistical analysis, methodology development.

References

[1] V.E. Privalov, V.G. Shemanin. Opt. Spectrosc., **130** (3), 331 (2022). DOI: 10.61011/EOS.2024.01.58283.6-24
[2] L.M. Narlagiri, M.S.S. Bharati, R. Beeram, D. Banerjee, V. Rao Soma. Trends Anal. Chem., **153**, 116645 (2022). DOI:10.1016/j.trac.2022.116645
[3] D.D. Tuschel, A.V. Mikhonin, B.E. Lemoff, S.A. Asher. Appl. Spectrosc., **64** (4), 425-32 (2010). DOI: 10.1366/000370210791114194
[4] C.S. Cockell, J. Knowland. Biol. Rev. Camb. Philos. Soc., **74** (3), 311−45 (1999). DOI: 10.1017/s0006323199005356
[5] M.O. Rodgers, K. Asai, D.D. Davis. Appl. Opt., **19** (21), 3597 (1980). DOI: 10.1364/AO.19.003597
[6] T. Arusi-Parpar, D. Heflinger, R. Lavi. Appl. Opt., **40** (36), 6677 (2001). DOI: 10.1364/AO.40.006677
[7] C. M. Wynn, S. Palmacci, R.R. Kunz, K. Clow, M. Rothschild. Appl. Opt., **47** (31), 5767 (2008). DOI: 10.1364/AO.47.005767
[8] D. Wu, J.P. Singh, F.Y. Yueh, D.L. Monts. Appl. Opt., **35** (21), 3998 (1996). DOI: 10.1364/AO.35.003998
[9] S.M. Bobrovnikov, E.V. Gorlov, V.I. Zharkov, Yu.N. Panchenko, A.V. Puchikin. Appl. Opt., **57**(31), 9381 (2018). DOI: 10.1364/AO.57.009381
[10] S.M. Bobrovnikov, E.V. Gorlov, V.I. Zharkov, Yu.N. Panchenko, A. Puchikin. Appl. Opt., **58**(27), 7497 (2019). DOI: 10.1364/AO.58.007497
[11] M.-F. Lin, Y.T. Lee, C.-K. Ni, S. Xu, M.C. Lin. J. Chem. Phys., **126**(6), 064310 (2007). DOI: 10.1063/1.2435351
[12] A.V. Puchikin, Yu.N. Panchenko, S.A. Yampolskaya, M.V. Andreev, V.E. Prokopiev. J. Lumin., **263**, 120073 (2023). DOI: 10.1016/j.jlumin.2023.120073
[13] J. Viallon, S. Lee, P. Moussay, K. Tworek, M. Petersen, R.I. Wielgosz. Atm. Meas. Tech., **8** (3), 1245 (2015). DOI: 10.5194/amt-8-1245-2015
[14] K.A. Rahman, K.S. Patel, M.N. Slipchenko, T.R. Meyer, Zh. Zhang, Y. Wu, J.R. Gord, S. Roy. Appl. Opt., **57** (20), 5666 (2018). DOI: 10.1364/AO.57.005666
[15] J.B. Schmidt, S. Roy, W.D. Kulatilaka, I. Shkurenkov, I.V. Adamovich, W.R. Lempert, J.R. Gord. J. Phys. D, **50** (1), 015204 (2017). DOI: 10.1088/1361-6463/50/1/015204
[16] M. Hay, P. Parajuli, W.D. Kulatilaka. Proc. Combust. Inst., **39**(1), 1435 (2023). DOI: 10.1016/j.proci.2022.08.090
[17] A.V. Puchikin, Yu.N. Panchenko, S.A. Yampolskaya, M.V. Andreev, V.E. Prokopiev. J. Lumin., **268**, 120412 (2024). DOI: 10.1016/j.jlumin.2023.120412
[18] Y.N. Panchenko, A.V. Puchikin, S.A. Yampolskaya, S.M. Bobrovnikov, E.V. Gorlov, V. I. Zharkov. IEEE J. Quant. Electron., **57** (2), 1 (2021). DOI: 10.1109/JQE.2021.3049579
[19] Yu.I. Bychkov, A.G. Yastremskii, S.A. Yampolskaya, V.F. Losev, V. Dudarev, Yu.N. Panchenko, A.V. Puchikin. Russ. Phys. J., **57** (7), 929 (2014). DOI: 10.1007/s11182-014-0326-3
[20] S.A. Yampolskaya, A.G. Yastremskii, Yu.N. Panchenko, A.V. Puchikin, S.M. Bobrovnikov. IEEE J. Quant. Electron., **56** (2), 1500209 (2020). DOI: 10.1109/JQE.2020.2976532
[21] J. Luque, D.R. Crosley. LIFBASE: Database and Spectral Simulation Program (Version 1.5), SRI International Report MP 99-009 (1999). https://www.sri.com/engage/products-solutions/lifbase
[22] W.G. Bessler, C. Schulz, V. Sick, J.W. Daily. Proc. Third Joint Meeting US Sec. Combust. Inst., **105**, 1 (2003). https://api.semanticscholar.org/CorpusID:92818989
[23] R.C. Reid, J.M. Prausnitz, T.K. Sherwood. *The Properties of Gases & Liquids* (Chem. Eng. Series, McGraw-Hill, NY., 1977).
[24] L. Frøsig, O.J. Nielsen, M. Bilde, T.J. Wallington, J.J. Orlando, G.S. Tyndall. J. Phys. Chem. A, **104** (48), 11328 (2000). DOI: 10.1021/jp002696o
[25] C. Tanjaroon, C.J. Lue, S.W. Reeve, S.D. Allen, J.B. Johnson. Chem. Phys. Lett., **641**, 33 (2015). DOI: 10.1016/j.cplett.2015.10.051
[26] Y.-M. Li, J.-L. Sun, H.-M. Yin, K.-L. Han, G.-Z. He. J. Chem. Phys., **118** (14), 6244 (2003). DOI: 10.1063/1.1557932
[27] D.B. Galloway, J.A. Bartz, L.G. Huey, F.F. Crim. J. Chem. Phys., **98**(3), 2107 (1993). DOI: 10.1063/1.464188

[28] K. Bogumil, J. Orphal, T. Homann, S. Voigt, P. Spietz, O.C. Fleischmann, A. Vogel, M. Hartmann, H. Bovensmann, J. Frerick, J.P. Burrows. J. Photochem. Photobiol. A, **157**(2-3), 167 (2003). DOI: 10.1016/S1010-6030(03)00062-5
[29] R.M. Measures. *Laser remote sensing: fundamentals and applications* (Krieger, Melbourne, 1992).
[30] D.B. Galloway, T. Glenewinkel–Meyer, J.A. Bartz, L.G. Huey, F.F. Crim. J. Chem. Phys., **100** (3), 1946 (1994). DOI: 10.1063/1.466547
[31] L.A. Melton, W. Klemperer. Planet. Space Sci., **20**(2), 157 (1972). DOI: 10.1016/0032-0633(72)90097-9
[32] A.B. Callear, M.J. Pilling. Trans. Faraday Soc., **66**, 1618 (1970). DOI: 10.1039/TF9706601618

Translated by E.Ilinskaya